

FOCUS: MICROSCOPY AND IMAGING

What Ticks Do Under Your Skin: Two-Photon Intravital Imaging of *Ixodes Scapularis* Feeding in the Presence of the Lyme Disease Spirochete

Linda K. Bockenstedt^{a*}, David Gonzalez^b, Jialing Mao^a, Ming Li^a,
Alexia A. Belperron^a and Ann Haberman^b

^aDepartment of Internal Medicine, Yale School of Medicine, New Haven, Connecticut;

^bDepartment of Laboratory Medicine, Yale School of Medicine, New Haven, Connecticut

Lyme disease, due to infection with the *Ixodes*-tick transmitted spirochete *Borrelia burgdorferi*, is the most common tick-transmitted disease in the northern hemisphere. Our understanding of the tick-pathogen-vertebrate host interactions that sustain an enzootic cycle for *B. burgdorferi* is incomplete. In this article, we describe a method for imaging the feeding of *Ixodes scapularis* nymphs in real-time using two-photon intravital microscopy and show how this technology can be applied to view the response of Lyme borrelia in the skin of an infected host to tick feeding.

*To whom all correspondence should be addressed: Linda K. Bockenstedt, MD, Harold W. Jockers Professor of Medicine, Section of Rheumatology, Department of Internal Medicine, Yale School of Medicine, 300 Cedar St., New Haven, CT 06520-8031; Tel: 203-785-2453; Fax: 203-785-7053; Email: linda.bockenstedt@yale.edu.

†Abbreviations: MyD88, myeloid differentiation primary response gene 88; TLR, Toll-like receptor; PBS, phosphate buffered saline; GFP, green fluorescent protein; FITC, fluorescein isothiocyanate; DAPI, diamidino-2-phenylindole.

Keywords: *Ixodes scapularis* ticks, two-photon intravital microscopy, *Borrelia burgdorferi*, Lyme disease

Author contributions: LK Bockenstedt conceived, designed and conducted the studies, and wrote the manuscript; D Gonzalez assisted with the study design and interpretation, conducted the studies, and edited the manuscript; J Mao, M Li, and AA Belperron conducted the studies and edited the manuscript; A Haberman assisted with study design and interpretation and edited the manuscript.

INTRODUCTION

In 1975, an unusual clustering of arthritis cases in the region of Lyme, Connecticut, led to the discovery of the emerging tick-borne zoonosis called Lyme disease [1]. The hallmark skin lesion erythema migrans that often predated the arthritis had been associated in Europe in the early 1900s with the bite of *Ixodes* species ticks and was presumed to be infectious in origin. Lyme disease is now known to be caused by infection with spirochetes of the *Borrelia burgdorferi sensu lato* complex and is the most common tick-borne disease in the northern hemisphere [2].

Hard-bodied ticks of the Ixodidae family are the only known vectors for Lyme borrelia and transmit the pathogen to the blood meal vertebrate host during feeding [2]. The enzootic cycle that maintains Lyme borrelia involves horizontal amplification by passage of the pathogen from a reservoir host to feeding ticks, as transovarial transmission from the adult tick to eggs does not routinely occur. All stages of Ixodid ticks must feed for several days to complete the blood meal. Efficient transfer of Lyme borrelia between the tick and the blood meal host and establishment of infection typically occurs only after 3 days of tick attachment [3]. During tick feeding, Lyme borrelia replicate in the tick midgut, pass through the hemolymph, and enter the salivary glands. From there, they pass with saliva into the bite site. From the skin inoculation site, spirochetes can spread contiguously through the dermis and/or disseminate through the blood to other tissues. As the blood-borne phase is transient, hematogenous dissemination is believed to permit widespread skin colonization, thereby enhancing acquisition of Lyme borrelia by ticks feeding on competent reservoir hosts to complete the enzootic cycle.

Our understanding of the vector-host-pathogen interactions that occur during *Ixodes* tick feeding have been derived largely from static images or assays conducted on the tick, the spirochete, or the vertebrate host at discrete points during the

infectious cycle. While much is known about the questing behavior of ticks seeking blood meal hosts [4], less is understood about the tick feeding process itself and the physical means by which tick-borne pathogens move between the tick and vertebrate host. Spirochetes within the tick midgut respond to tick feeding by activating the Rrp2-RpoN-RpoS pathway that regulates the expression of proteins required for mammalian survival, including the outer membrane protein (Osp) C, numerous adhesins that promote binding to the extracellular matrix components, and proteins that aid in evasion of complement-mediated lysis [5]. This pathway remains activated in the mammalian host and as spirochetes return to feeding ticks [6]. Successful establishment of infection within a feeding tick requires de-repression of the Hk1-Rrp1 pathway that controls expression of tick-phase genes such as OspA, a tick midgut adhesion [7,8]. Despite delineation of these pathways and identification of proteins required for infection in the mammal or tick, the precise role that many of these proteins play in the transitioning of Lyme borrelia between the tick and the mammal remains unclear. A system capable of simultaneously imaging Lyme borrelia in the skin and a feeding tick in real-time may provide a tool to enhance our understanding of this aspect of Lyme borrelia biology.

Using *Ixodes ricinus* nymphs, the primary vector for Lyme borrelia in Europe, a recent study has elegantly demonstrated in real-time how ticks insert their mouthparts to anchor themselves to the vertebrate host [9]. The study employed cinematography to visualize a tick inserting its mouthparts into the skin barrier and scanning electron microscopy and confocal microscopy to define the feeding apparatus structure. From these imaging techniques, a model was developed to explain how the chelicera movements visualized could anchor the tick to the host. Herein, we expand on this study to describe a method for visualizing, using two-photon intravital microscopy, the movement of the mouthparts after they have been inserted into the mouse dermis. We also show how

this technique can be applied to study the response of mammalian-adapted Lyme borreliosis to a feeding tick.

MATERIALS AND METHODS

Spirochetes

Two previously described green fluorescent protein (GFP⁺)-expressing transformants of *B. burgdorferi sensu stricto* were used in this study. The transformant KS41 was derived from *B. burgdorferi* strain B31-5A-14, a clonal subculture of strain B31-MI, and was generously provided by Brian Stevenson (University of Kentucky, Louisville, KY) [10]. KS41 has been shown to readily pass between mice and ticks and can sustain infection for at least 6 months in mice [11]. The GFP-expressing stable transformant of *B. burgdorferi* strain 297 (Bb914) was kindly provided by Melissa Caimano (University of Connecticut Health Center, Farmington, CT) [12]. This transformant is infectious to ticks and mice with similar dynamics of transmission as the parent strain 297 [12]. Frozen stocks of low passage KS41 or Bb914 were thawed and expanded in Barbour Stoenner Kelley II medium immediately prior to use. Mice were infected by intradermal inoculation of 10^4 spirochetes or by infestation with *B. burgdorferi*-infected nymphs as described [13].

Mice

C57BL/6J WT were obtained from The Jackson Laboratory (Bar Harbour, ME). Breeding pairs of C57BL/6J myeloid differentiation primary response gene 88 (MyD88)^{-/-} mice, originally produced by Shizua Akira [14], and Balb/c *rag*^{-/-} mice originally purchased from Taconic Labs (Germantown, NY) were obtained from Mark Shlomchik (previously at Yale University), and both strains were maintained as a colony. All mice were housed according to Yale Animal Care and Use Guidelines in specific pathogen-free rooms with autoclaved food, water, and bedding. Mice were relocated to a dedicated BL2 facility for experiments. MyD88^{-/-} mice were provided sulfamethoxazole-trimethoprim 0.25 mg/ml

in drinking water (Sulfatrim, Sigma-Aldrich) to reduce the risk for opportunistic infection. This antibiotic has no effect on *B. burgdorferi* infection in mice or ticks. Mice were killed by carbon dioxide asphyxiation. All animal studies and procedures were approved by the Yale Animal Care and Use Committee.

Ticks

Specific pathogen-free laboratory-reared *Ixodes scapularis* nymphs were obtained from Durland Fish (Yale School of Medicine, New Haven, CT). Nymphs infected with Bb914 at the time of larval stage feeding were produced as previously described [13].

Tick Infestation of Mice

Mice were mildly anesthetized with ketamine (100 mg/kg) and xylazine (10 mg/kg) to permit immobilization for tick placement and attachment. Up to four nymphs were placed on the ears of mice and observed to attach. Mice were observed until they regained consciousness and then were singly housed in cages with triple barriers for tick containment according to procedures approved by the Yale Animal Care and Use Committee.

Intravital Microscopy

Real-time imaging of tick feeding was performed using an upright multiphoton laser scanning microscope outfitted with a Chameleon Vision II Ti:Sapphire Laser (Coherent) with pulse precompensation. An array of images were acquired using an Olympus BX61 WI fluorescence microscope with a $\times 20$, 0.95NA water immersion Olympus objective and dedicated single-beam LaVision TriM scanning laser (LaVision Biotec) that was controlled by Inspector software. Emission wavelengths of three photomultiplier tubes collected emission wavelengths at 390-480 nm (blue), 500-550 nm (green, GFP), and 565-665 nm (orange-red). Mice were anesthetized with an intraperitoneal injection of ketamine (100 mg/kg) and xylazine (10 mg/kg) to prep the imaging site and for placement on a stereo-

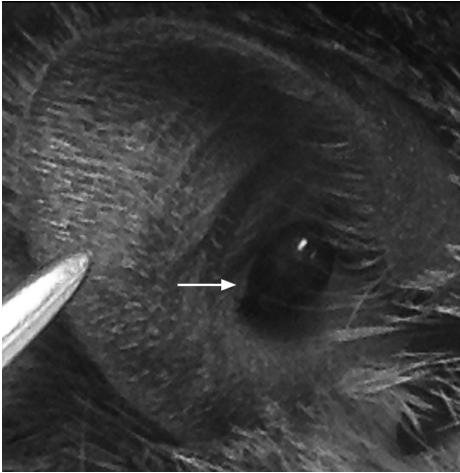


Figure 1. Engorged *Ixodes scapularis* nymphs attached to ear pinnae for two-photon imaging. The location of the tick is ideal for live imaging.

taxic restraint platform. Hair in the region of the imaging site was removed using the topical depilatory Nair, after which the area was rinsed with phosphate buffered saline (PBS). During imaging, a deep plane of anesthesia was maintained using a mixture of isoflurane gas and oxygen delivered using a nosecone. Image stacks of ≤ 15 optical sections with 2- to 3- μm z-spacing were acquired every 20 to 25 seconds for 60 to 120 minutes with the laser tuned to a wavelength of 875-940 nm. Each xy plane spanned 300-500- μm in each dimension with a resolution of 1.17-0.59 μm per pixel. Volocity software (Improvision) was used to create Quick-Time-formatted videos of image sequences. All videos are displayed as 2D maximum intensity projections, unless otherwise stated.

Immunofluorescence Staining of Lyme Borrelia in Mouse Skin

After imaging and mouse sacrifice, ear pinnae were removed and flash frozen in OCT compound for sectioning. Six μm cryosections were fixed in acetone, air dried, then blocked for 30 minutes with PBS containing 5 percent goat serum. Sections were stained with a 1:30 dilution of FITC-conjugated polyclonal antibody to *B. burgdorferi* (KPL Inc.), and nuclei were labeled with DAPI (1 μg final concentration, Sigma-Aldrich). After rinsing twice in PBS, slides

were air dried prior to mounting coverslips with Fluoromount G. Tissue sections were visualized at 400X magnification using an Olympus BX40 widefield immunofluorescence microscope equipped with digital imaging.

RESULTS

Optimization of Tick Placement

In mice, the ear is well suited for live imaging of the skin because it provides an easily accessible, relatively flat surface for microscopy. In order to image tick feeding without the need for disrupting the skin integrity, nymphs were placed on the central inner aspect of the external ear (Figure 1, shown for an engorged tick). After various periods of time, from 4 hours to 5 days, mice were prepped for imaging the opposite (external) side of the ear. Prior to mounting the mouse on the stereotactic platform, the side of the ear with the exposed tick body was adhered using surgical glue to a metal dowel with an engraved depression to accommodate the tick body (Figure 2a). The dowel was mounted onto a custom-designed stereotactic platform in the desired position using modeling clay (Figure 2b). A drop of PBS was placed on the depilated skin to wet the surface to be imaged and to provide a consistent medium for light to transmit to the objective. A round glass coverslip anchored to a micromanipulator was lowered onto the ear, creating a flat imaging surface. A metal loop was placed on top of the coverslip with vacuum grease to create a well for water into which the objective could be lowered (Figure 2c).

Motions of the Mouthparts During Attachment and Feeding

We first established that we could visualize the components of the feeding apparatus through the layers of the skin after the tick had attached to the ear skin. Scanning electron microscopy images of an *Ixodes scapularis* nymph delineated the dorsal view of the feeding apparatus with the finger-like chelicera (Figure 3a,b) and their relationship

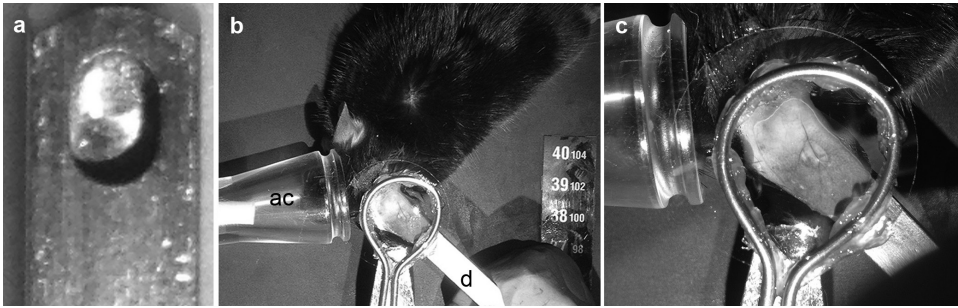


Figure 2. Preparation of the tick bite site for two-photon imaging. The side of the mouse ear with the exposed tick body is glued to a metal dowel with a depression large enough to accommodate an engorged tick body. **a)** After placement of the anesthetized mouse on the imaging stage, the dowel can be fixed in appropriate position using modeling clay (**b**) d= dowel, ac = anesthesia cone). **c)** A coverslip is placed over the imaging site and a wire loop is adhered to the surface to contain water required for the water immersion lens.

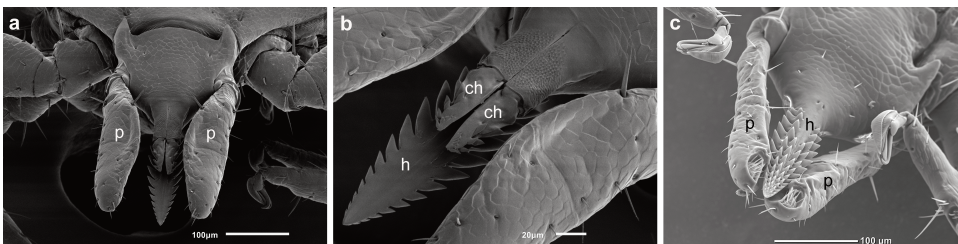


Figure 3. Scanning electron micrographs of the feeding apparatus of an *Ixodes scapularis* nymph. **a)** Dorsal view of the tick head with palps (p) flanking the mouthparts. **b)** Dorsal view of the mouthparts, revealing the hypostome (h) and chelicerae (ch). **c)** Ventral view of the hypostome (h) and adjacent palps (p). Images were acquired using a JOEL JSM-6010LA scanning electron microscope (JOEL, USA).

to the barbed ventral surface of the hypostome (Figure 3c). The chitinous hard shell of the tick and feeding apparatus was brightly autofluorescent when visualized by two-photon microscopy (Figure 4a), and both the hypostome and its tooth-like denticles and the chelicera appendages (when extended) were readily apparent (Figure 4a,b). At 72 hours, the tissue surrounding the hypostome had evolved a cone-like structure, which appeared to exclude blood that had extravasated into the tissue from the wound. This cone formation may be due to a reorganization of the collagen matrix at the feeding site (Figure 4a, Supplementary Movie 1).

A recent study has reported that the insertion of the hypostome into the skin occurs via a ratcheting mechanism in which the chelicerae extend into the skin and retract in a breaststroke-like movement, thereby propelling the hypostome forward [9]. Early on during the attachment process (within 1 to 4

hours), we observed that the hypostome stabbed deeper into the dermis at times when the chelicerae were not visible, consistent with this mechanism (Supplementary Movie 2). Chelicera motion occurred at all time points in which the tick was observed to feed, but chelicera extended in a slightly asynchronous fashion when observed after 24 hours of tick attachment (Supplementary Movies 3-5).

Visualizing Effects of Feeding Ticks on *Lyme Borrelia* in Infected Mice

The ability to visualize tick feeding in real-time afforded us an opportunity to observe how *Lyme borrelia* within the mammal respond to the presence of a feeding tick. To improve our ability to visualize numerous spirochetes in a single visual field, we initially conducted these studies in mice deficient in either adaptive immunity (*rag*^{-/-} mice) or the Toll-like receptor (TLR) adaptor molecule MyD88. All TLRs that respond

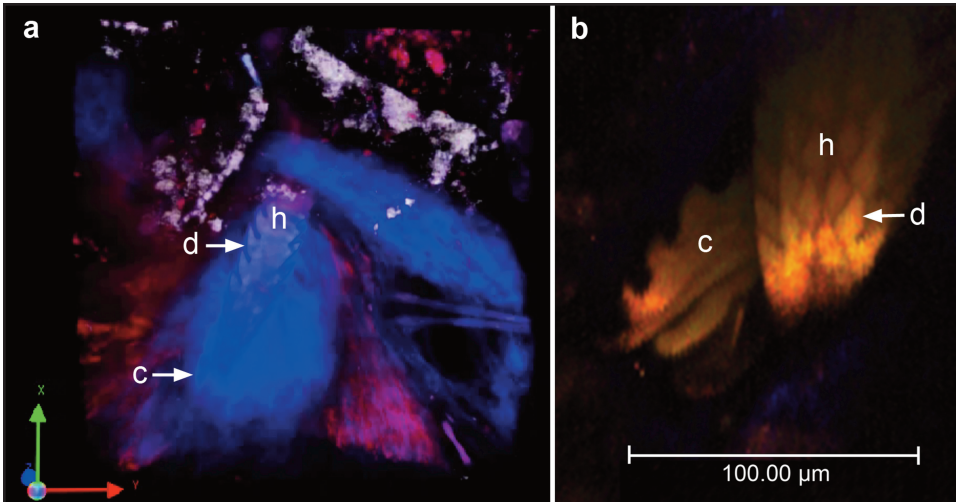


Figure 4. Snapshots of two-photon images of the mouthparts after insertion into the dermis. **a)** Snapshot of Z-stack movie of the skin bite site at 72 hours of tick attachment. The 3-dimensional z-stack image was rendered using Volocity software from images of sequential xy planes taken at different levels in the tissue. Note the dense cone-shaped appearance of the blue collagen fibers surrounding the hypostome. These fibers appear blue due to second harmonic generation. Rhodamine-conjugated dextran was injected intravenously prior to imaging to demonstrate the extravasation of blood adjacent to the hypostome. **b)** Ventral aspect of the hypostome with a single chelicera extended. h = hypostome, c = chelicera, d = denticle.

to Lyme borrelia utilize MyD88 to transduce signals and interruption of this pathway through genetic deletion of MyD88 results in pathogen burdens as much as 100-fold more than what typically occurs in infection of wild type mice [15,16]. *B. burgdorferi* infection of mice deficient in B cells, such as *rag*^{-/-} mice, also exhibit elevated pathogen burden [17]. Mice infected with a GFP-expressing Lyme borrelia (Bb914 or KS41) for at least 2 weeks were used as blood meal hosts for nymphs. Motility patterns of Bb914 and KS41 in the dermis are similar with several types of motion observed: wriggling, in which spirochetes undulate as a traveling wave but do not advance in any direction; lunging, in which spirochetes are fixed at one end and the other end is intermittently thrust away from the fixed end; and translocating, in which spirochetes oscillate back and forth along dermal collagen fibers or travel directionally [18,19]. These motility patterns are identical in wild type, *rag*^{-/-}, and MyD88-deficient mice [19]. In response to tick feeding, we noted that some spirochetes remain wriggling in place,

whereas others appear to move toward the hypostome region and disappear (Supplementary Movie 4, Figure 5). We were unable to visualize spirochetes as they neared the tick hypostome, possibly because of optical interference of fluids within the cone-shaped feeding site. When moving toward the hypostome, spirochetes tended to follow similar paths (Supplementary Movie 4). Directional translocation of spirochetes toward the feeding tick was also observed when wild type mice were used as blood meal hosts (Supplementary Movie 5). We noted that spirochetes approached the feeding tick as early as 6 hours after attachment, the earliest time point examined in these studies (data not shown).

We also attempted to visualize GFP-labeled *B. burgdorferi* as they were deposited by feeding ticks into the blood meal host. Despite imaging at days 1, 2, 3, 4, and 5 after tick attachment to wild type or MyD88^{-/-} hosts, we did not detect GFP⁺ spirochetes in the vicinity of the feeding pit, nor did we capture images of GFP⁺ material exiting the tick. All ticks used for transmission studies

were infected when midguts were examined by immunofluorescence staining for spirochetes and by PCR for spirochete DNA (data not shown). When the skin was examined post mortem, we were not able to find spirochetes by immunofluorescence staining except once at day 5 (Figure 6a). By day 7 after initial tick placement and usually 2 to 3 days after the tick had completed its blood meal and detached, spirochetes were readily visualized at this site (Figure 6b).

DISCUSSION

Ixodes ticks are obligate blood-sucking ectoparasites that require extended periods (days) of attachment to vertebrate hosts to complete the blood meal [20]. This prolonged period of feeding is an advantage when applying novel imaging techniques to study vector-host interactions. Our study demonstrates that two-photon intravital microscopy can be used to directly observe the physical interactions of a feeding *Ixodes scapularis* nymph with the murine blood meal host in real-time with minimal perturbation of either the tick or the mouse. Two-photon confocal microscopy permits imaging to greater depths with less phototoxicity to tissues when compared to conventional confocal microscopy and has been used to image immune events associated with vector-associated pathogens [21]. These microscopy features are particularly advantageous when imaging tick feeding as they allow visualization of the mouthparts inserted in ear skin without surgical exposure of the bite site. The autofluorescence of the tick shell and second harmonic generation of the collagen fibers within the dermis allow visualization of both the tick and the dermis without the need for fluorescent labeling. Although we typically acquired images over a period of an hour or so, two-photon microscopy can be used to repetitively sample an area over significantly longer periods of time.

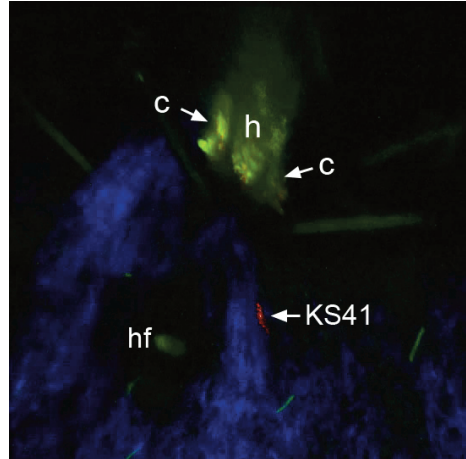


Figure 5. Snapshot of *Ixodes scapularis* nymph 48 hours after attachment to the ear of a mouse infected with the GFP-expressing spirochete KS41. Several spirochetes can be seen in the visual field. A representative KS41 spirochete observed to move toward the hypostome during the imaging period was digitally labeled in red (see Supplementary Movie 4). h= hypostome, c = chelicera, hf = hair follicle.

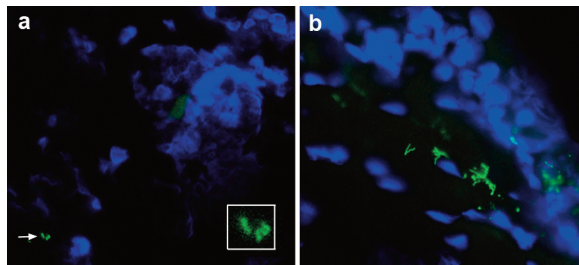


Figure 6. Direct immunofluorescence of *B. burgdorferi* in ear skin after tick feeding. **a)** Rare spirochete forms (green) are seen in the dermis (arrow) at day 5 after tick attachment (enlarged in insert). Skin cell nuclei (blue) are stained with DAPI. The tick had spontaneously detached prior to this analysis. **b)** Spirochetes are more numerous at day 7 after tick attachment (the tick had detached on day 4).

Two-photon intravital microscopy allowed us to provide live imaging support for proposed actions of the components of the feeding apparatus as the tick penetrates the skin barrier and extend the findings published previously [9,22]. The *Ixodes* hypostome, comprised of the barbed dentition on the ventral surface and the cheliceral cutting digits on the dorsal side, is of sufficient length that it can penetrate well into the der-

mis of mice, obviating the need for cementing the feeding apparatus to the skin [22]. Indeed, although the *Ixodidae* family of ticks has evolved to secrete proteins that form a cement plug to anchor the mouthparts, this adaptation is not conserved among all *Ixodes* species. The chelicerae cut into the skin using breaststroke-like motions that propel the hypostome deep beneath the surface through a ratchet-like motion [22]. Our two-photon imaging studies revealed an episodic thrusting of the hypostome at times when the chelicera were not extended, consistent with this mechanism.

Once attached to the skin, we observed significant reorganization of the collagen fibers surrounding the hypostome over time. By 72 hours of attachment, the fibers appeared to form a cone surrounding the hypostome, delineating a lucent region immediately adjacent to the hypostome. This area may be filled with interstitial fluid and/or blood. We also observed that the chelicerae continue to churn the contents of this lucent area. *Ixodes* tick feeding involves successive waves of expulsion of saliva into the bite site interspersed with aspiration of the contents [23]. Mixing of the fluids around the bite site may facilitate collagen reorganization into the cone-like structure surrounding the hypostome and continually disperse the pharmacologically active components of tick saliva that impair wound healing, suppress coagulation, and diminish immune defenses [24]. Interestingly, at the 72-hour time point, only traces of blood were seen in the feeding site near the hypostome, suggesting that collagen reorganization may help the tick adjust the intensity of the blood flow during feeding.

Our live imaging captured several facets of the chelicera in motion. When viewed end-on, as in Supplementary Movie 3, the coordinated splaying of the cheliceral digits can be readily appreciated, along with their retraction without significant repulsion of the hypostome. The hooked digit can be seen in Figure 4b, and its movement in Supplementary Movie 5 suggests that it may serve not only to anchor the chelicera once extended, but also to force back collagen fibers that may compress the feeding site.

Our group has previously reported the use of two-photon intravital microscopy to image live Lyme borrelia within mammalian tissues after infection has been introduced by feeding ticks or by needle inoculation of cultured spirochetes [18,19]. We observed that mammalian adapted spirochetes are heterogeneous with respect to their motility patterns in the dermis during the disseminated and persistent phases of infection. Thus, while Lyme borrelia undergo global changes in gene expression in response to environmental cues associated with their transition to the mammalian or tick environment, once adapted to the host, they exhibit differential responses to local stimuli. In the current study, mice had been infected with *B. burgdorferi* for 2 weeks prior to tick infestation, a time when they were fully mammalian adapted and had disseminated from the initial inoculation skin site to multiple areas of the skin. Although some spirochetes within the dermis were observed to move toward the hypostome during the 1-hour imaging period, others appeared oblivious to the tick presence. Spirochete movement is unlikely to be due simply to the mechanical flux of tissue fluid as the tick feeds because close examination of individual spirochetes that move toward the hypostome reveals both the oscillating movements that we observe in the absence of tick feeding as well as directional translocation. Presumably, factors within tick saliva signal de-repression of the Hk1-Rrp1 pathway in *B. burgdorferi* that regulates tick phase genes even though the Rrp2-RpoN-RpoS pathway that controls the mammalian phase gene program may still be engaged [5,6]. How rapidly an individual spirochete responds to tick feeding is likely related to multiple factors, including its location relative to the hypostome and gradient of tick saliva as well as its environmental sensing that induces a tick phase gene program. Our finding that some spirochetes move toward the hypostome as early as 6 hours after tick attachment suggests that this sensing can occur relatively quickly, although successful entry into and retention by the feeding tick has only been demonstrated by immunofluorescent staining of tick midgut contents after 12 hours of attachment [25].

Transmission of Lyme borrelia from feeding ticks to the murine host has been observed by immunofluorescence of mouse skin at the bite site as early as 42 hours after tick attachment [26]. Successful infection of the mammal, however, usually occurs after 72 hours of feeding. The numbers of spirochetes that are transmitted by a fully engorged tick are quite low (estimated to be in the hundreds). We therefore expected that two-photon imaging would reveal a few spirochetes near the hypostome by 72 hours of tick feeding. Our inability to visualize spirochetes in the dermis at time intervals up to 5 days after attachment of infected ticks suggests that spirochetes transmitted remain localized within the lucent zone surrounding the hypostome, an area not resolved by our imaging. Our inability to detect spirochetes by two-photon microscopy was supported by immunofluorescence staining of the tissues, in which we were unable to detect *B. burgdorferi* until day 5 after tick attachment. This significant delay reflects the fact that spirochetes transmitted by feeding ticks are only partially host adapted. RpoS induction of proteins involved in the mammalian phase of infection is only completed in the mammal itself [5,27]. It is possible that longer periods of imaging may allow visualization of a rare spirochete that is deposited in the bite site. Our findings confirm that despite massive expansion of spirochete numbers in feeding ticks, there are significant barriers within the tick that permit only a few highly selected spirochetes to enter the vertebrate host.

Xenodiagnosis, a process in which the vector for a pathogen is used to detect infection, has been proposed as a method to study Lyme disease in humans [28,29]. *Ixodes* larvae and nymphs are fully capable of retrieving viable spirochetes from laboratory mice infected with *B. burgdorferi*. This is possible because inbred mice are competent reservoir hosts for Lyme borrelia and can serve as surrogates for the natural reservoir host, *Peromyscus leucopus* (the white-footed mouse) [2]. Our studies using two-photon microscopy support the prevailing notion that feeding ticks acquire *B. burgdorferi* from the skin, not from the

blood. Thus, in order for xenodiagnosis to aid in the detection of human infection with *B. burgdorferi* when the hallmark erythema migrans lesion is no longer present, the pathogen must be able to disseminate and persist in human skin in sufficient numbers so that random placement of ticks may acquire them [29].

Our procedure for imaging tick feeding in real time has some technical limitations. First, nymphal ticks must be observed to attach at a desired location on the flat surface of the ear pinnae to optimize imaging. At this location, the skin is thin and occasionally nymphal ticks will extend their hypostomes through the full thickness of the skin, piercing the opposite side. Mice must remain in a deep plane of anesthesia throughout the imaging period to minimize the discomfort of prolonged immobilization, during which time they must be kept warm to prevent vasoconstriction that may interfere with tick feeding. Most importantly, the actions of the chelicerae create motion artifact that can compromise image acquisition and resolution.

In summary, two-photon intravital microscopy is a powerful tool that can be applied to the study of certain vector-borne zoonoses, particularly those in which the interaction of the vector with the vertebrate host occurs over a period of several hours to days. The ability to simultaneously image *Ixodes* tick feeding, Lyme borrelia, and the vertebrate in real time will enable the construction of models that more accurately depict the spatial and temporal interactions that complete the enzootic cycle of *B. burgdorferi*. Future studies employing this form of microscopy may help enlighten the fundamental processes that govern arthropod-borne zoonoses like Lyme disease.

SUPPLEMENTARY MATERIAL

Supplementary Movie 1. Z-stack of tick bite site 72 hours after tick attachment. Imaging parameters: scanfield dimension = 500 μm^2 , wavelength = 875, pixel resolution = 1024, Z-step = 2 μm , optical sections = 15.

Supplementary Movie 2. Hypostome propulsion into skin. Imaging parameters: scanfield dimension = 300 μm^2 , wavelength = 880 nm, pixel resolution = 256, Z-step = 3 μm , optical sections = 15.

Supplementary Movie 3. Feeding apparatus end-on with cheliceral movement. One-hour movie. Imaging parameters: scanfield dimension = 400 μm^2 , wavelength = 940 nm, pixel resolution = 512, Z-step = 3 μm , optical sections = 15.

Supplementary Movie 4. *Ixodes scapularis* nymph feeding on GFP-Lyme borrelia-infected wild type mouse. One-hour movie. Imaging parameters: scanfield dimension = 300 μm^2 , wavelength = 940 nm, pixel resolution = 512, Z-step = 3 μm , optical sections = 15.

Supplementary Movie 5. *Ixodes scapularis* nymph feeding on GFP-Lyme borrelia-infected *rag-/-* mouse at 48 hours. One-hour movie. A representative spirochete moving toward the hypostome is highlighted in red. The rendering to change the color of the pixels making up a spirochete reduces the resolution of the spirochete itself. Imaging parameters: scanfield dimension = 500 μm^2 ; wavelength = 940 nm; pixel resolution = 512; Z-step = 2 μm ; optical sections = 15.

Acknowledgments: This work was supported by NIH P30AR053495 (LKB and AH), R01AI085798 (LKB), a pilot grant from The National Research Fund for Tick-Borne Diseases (LKB), and the Harold W. Jockers Professorship (LKB). The authors thank Ms. Rebecca L. Fine for excellent assistance with graphics and JOEL, USA for producing the scanning electron micrographs of an *Ixodes scapularis* nymph.

REFERENCES

1. Steere AC, Malawista SE, Snyderman DR, Shope RE, Andiman WA, Ross MR, et al. Lyme arthritis: an epidemic of oligoarticular arthritis in children and adults in three connecticut communities. *Arthritis Rheum.* 1977;20(1):7-17.
2. Kurtenbach K, Hanincova K, Tsao JI, Margos G, Fish D, Ogden NH. Fundamental processes in the evolutionary ecology of Lyme borreliosis. *Nat Rev Microbiol.* 2006;4(9):660-9.
3. Piesman J, Mather TN, Sinsky RJ, Spielman A. Duration of tick attachment and *Borrelia burgdorferi* transmission. *J Clin Microbiol.* 1987;25(3):557-8.
4. Randolph SE. Tick ecology: processes and patterns behind the epidemiological risk posed by ixodid ticks as vectors. *Parasitology.* 2004;129:S37-S65.
5. Radolf JD, Caimano MJ, Stevenson B, Hu LT. Of ticks, mice and men: understanding the dual-host lifestyle of Lyme disease spirochaetes. *Nat Rev Microbiol.* 2012;10(2):87-99.
6. Dunham-Ems SM, Caimano MJ, Eggers CH, Radolf JD. *Borrelia burgdorferi* requires the alternative sigma factor RpoS for dissemination within the vector during tick-to-mammal transmission. *PLoS Pathog.* 2012;8(2):e1002532.
7. Caimano MJ, Kenedy MR, Kairu T, Desrosiers DC, Harman M, Dunham-Ems S, et al. The hybrid histidine kinase Hk1 is part of a two-component system that is essential for survival of *Borrelia burgdorferi* in feeding *Ixodes scapularis* ticks. *Infect Immun.* 2011;79(8):3117-30.
8. Pal U, Li X, Wang T, Montgomery RR, Ramamoorthi N, Desilva AM, et al. TROSPA, an *Ixodes scapularis* receptor for *Borrelia burgdorferi*. *Cell.* 2004;119(4):457-68.
9. Richter D, Matuschka FR, Spielman A, Mahadevan L. How ticks get under your skin: insertion mechanics of the feeding apparatus of *Ixodes ricinus* ticks. *Proc Biol Sci.* 2013;280(1773):20131758.
10. Miller JC, von Lackum K, Woodman ME, Stevenson B. Detection of *Borrelia burgdorferi* gene expression during mammalian infection using transcriptional fusions that produce green fluorescent protein. *Microb Pathog.* 2006;41(1):43-7.
11. Miller JC, Stevenson B. *Borrelia burgdorferi* erp genes are expressed at different levels within tissues of chronically infected mammalian hosts. *Int J Med Microbiol.* 2006;296(Suppl 40):185-94.
12. Dunham-Ems SM, Caimano MJ, Pal U, Wolgemuth CW, Eggers CH, Balic A, et al. Live imaging reveals a biphasic mode of dissemination of *Borrelia burgdorferi* within ticks. *J Clin Invest.* 2009;119(12):3652-65.
13. Bockenstedt LK, Mao J, Hodzic E, Barthold SW, Fish D. Detection of attenuated, noninfectious spirochetes in *Borrelia burgdorferi*-infected mice after antibiotic treatment. *J Infect Dis.* 2002;186:1430-7.
14. Adachi O, Kawai T, Takeda K, Matsumoto M, Tsutsui H, Sakagami M, et al. Targeted disruption of the MyD88 gene results in loss of IL-1- and IL-18-mediated function. *Immunity.* 1998;9:143-50.
15. Liu N, Montgomery RR, Barthold SW, Bockenstedt LK. Myeloid differentiation antigen 88 deficiency impairs phagocytosis but does not alter inflammation in *Borrelia burgdorferi*-infected mice. *Infect Immun.* 2004;72:3195-203.
16. Bolz DD, Sundsbak RS, Ma Y, Akira S, Kirschning CJ, Zachary JF, et al. MyD88 plays a unique role in host defense but not arthritis development in Lyme disease. *J Immunol.* 2004;173:2003-10.
17. Kang I, Barthold SW, Bockenstedt LK. Lyme borreliosis in B cell-deficient mice. *Arthritis Rheum.* 1995;38:S345.

18. Harman MW, Dunham-Ems SM, Caimano MJ, Belperron AA, Bockenstedt LK, Fu HC, et al. The heterogeneous motility of the Lyme disease spirochete in gelatin mimics dissemination through tissue. *Proc Natl Acad Sci USA*. 2012;109(8):3059-64.
19. Bockenstedt LK, Gonzalez DG, Haberman AM, Belperron AA. Spirochete antigens persist near cartilage after murine Lyme borreliosis therapy. *J Clin Invest*. 2012;122(7):2652-60.
20. Apanaskevich DA, Oliver JH. Life cycles and natural history of ticks. In: Sonenshine DE, Roe RM, editors. *Biology of Ticks*. Volume 1. 2nd edition. New York: Oxford University Press; 2014. p. 59-73.
21. Chong SZ, Evrard M, Ng LG. Lights, Camera, and Action: Vertebrate skin sets the stage for immune cell interaction with arthropod-vectored pathogens. *Front Immunol*. 2013;4:286.
22. Kemp DH, Stone BF, Binnington KC. Tick attachment and feeding: Role of the mouthparts, feeding apparatus, salivary gland secretions and the host response. In: Obenchain FD, Galun R, editors. *Physiology of Ticks*. Volume I. Elmsford, NY: Pergamon Press; 1982. p. 119-68.
23. Nosek J, Rajcani J, Kozuch O. Reaction of the host to the tick bite III. The bite of viruliferous *Ixodes ricinus* female. *Zentralblatt für Bakteriologie, Parasitenkunde, Infektionskrankheiten und Hygiene Erste Abteilung Originale Reihe A: Medizinische Mikrobiologie und Parasitologie*. 1978;242(2):141-7.
24. Ribeiro JMC, Franchischetti IMB. Role of arthropod saliva in blood feeding: Sialome and post-sialome perspectives. *Ann Rev Entomol*. 2003;48:73-88.
25. Schwan TG, Piesman J. Temporal changes in outer surface proteins A and C of the Lyme disease-associated spirochete, *Borrelia burgdorferi*, during the chain of infection in ticks and mice. *J Clin Microbiol*. 2000;38(1):382-8.
26. Ohnishi J, Piesman J, de Silva AM. Antigenic and genetic heterogeneity of *Borrelia burgdorferi* populations transmitted by ticks. *Proc Natl Acad Sci USA*. 2001;98(2):670-5.
27. Caimano MJ, Iyer R, Eggers CH, Gonzalez C, Morton EA, Gilbert MA, et al. Analysis of the RpoS regulon in *Borrelia burgdorferi* in response to mammalian host signals provides insight into RpoS function during the enzootic cycle. *Mol Microbiol*. 2007;65(5):1193-217.
28. Marques A, Telford SR III, Turk S-P, Chung E, Williams C, Dardick K, et al. Xenodiagnosis to detect *Borrelia burgdorferi* infection: A first-in-human study. *Clin Infect Dis*. 2014. In Press.
29. Bockenstedt LK, Radolf JD. Xenodiagnosis for posttreatment Lyme disease syndrome: resolving the conundrum or adding to it? *Clin Infect Dis*. 2014. In Press.